Accepted Manuscript

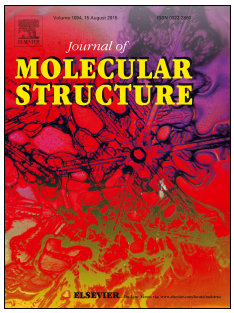

Sulfonated starch nanoparticles: An effective, heterogeneous and bio-based catalyst for synthesis of 14-aryl-14-*H*-dibenzo[a,j]xanthenes

Javad Safari, Pegah Aftabi, Majid Ahmadzadeh, Masoud Sadeghi, Zohre Zarnegar

PII: S0022-2860(17)30254-5

DOI: 10.1016/j.molstruc.2017.02.095

Reference: MOLSTR 23489

To appear in: *Journal of Molecular Structure*

Please cite this article as: Javad Safari, Pegah Aftabi, Majid Ahmadzadeh, Masoud Sadeghi, Zohre Zarnegar, Sulfonated starch nanoparticles An effective, heterogeneous and bio-based catalyst for synthesis of 14-aryl-14-H-dibenzo(a,j)xanthenes, *Journal of Molecular Structure* (2017), doi: 10.1016/j.molstruc.2017.02.095

Highlights

- Preparation of sulfonated starch nanoparticles (SO_3H-SNPs) as catalyst for organic synthesis.
- Introducing an efficient new catalyst for the synthesis of xanthenes.
- Excellent yields of products and short reaction times.

Sulfonated starch nanoparticles: An effective, heterogeneous and bio-based catalyst for synthesis of 14-aryl-14-*H*-dibenzo[a,j]xanthenes

Javad Safari*, Pegah Aftabi, Majid Ahmadzadeh, Masoud Sadeghi, Zohre Zarnegar

Laboratory of Organic Compound Research, Department of Organic Chemistry, College of Chemistry, University of Kashan, P.O. Box: 87317-51167, Kashan, I.R., Iran.

Abstract

In recent years, biodegradable polymer based nanoparticles have attracted wide attention for the synthesis of high-performance and green catalytic species. Polymeric nanoparticles used for catalytic processes must be biocompatible and biodegradable. The objective of this study is to fabricate starch nanoparticles from native starch and preparation of sulfonated starch nanoparticles (HO_3S-SNPs) as acidic nanocatalyst in the synthesis of 14-aryl-14-*H*-dibenzo[a,j]xanthenes under solvent free conditions. This procedure has a lot of advantages such as very easy reaction conditions, low-cost production and natural catalyst and absence of any tedious workup or purification. The corresponding products have been obtained in excellent yields, high purity and short reaction times.

Keywords: Sulfonated starch, Starch nanoparticles, Heterogeneous catalysis, 14-Aryl-14*H*-dibenzo[a,j]xanthenes, Solvent-free conditions.

1. Introduction

Homogeneous inorganic acids such as H_2SO_4 and HF are essential and efficient catalysts for the production of industrial important chemicals. However, the use of these homogeneous catalysts requires costly and inefficient processes for separation, recycling, and treatment of the spent acids. For example, the neutralization of the H_2SO_4 produces sulfate wastes, and

*Corresponding author. E-mail addresses: safari@kashanu.ac.ir; safari_jav@yahoo.com. Tel: +98 31 5591 2320; Fax: +98 31 5591 2397.

thus, the liquid acids do not fulfill the general requirement of a catalyst as a reusable material in chemical processes. The use of recyclable strong solid acids instead of unrecyclable homogeneous catalysts is a major area of research for the development of cleaner and more efficient processes [1-3].

Recently, the utilization of polymer bound catalysts is well recognized because of their ease of workup, simple and clean separation of products and catalysts from the reaction mixture. In this context, cellulose and starch are good candidates as natural, renewable, biocompatible, and biodegradable polymers [4-6]. As an ideal support material for catalysts, starch has unique properties including availability, safety, non-toxicity, and inexpensive and compatibility with many other materials. Owing to these properties, starch has been used as a bio-based support for a wide range of catalytic species. This catalyst gained much attention due to the low-cost production, easy preparation process, high effectiveness, greener and suitable for chemical transformations [4-8]. The polar hydroxyl groups in starch provide active sites for numerous attractive chemical modifications [3]. One such modification is sulfonation which leads to the formation of starch-SO_3H. Starch-SO_3H has been utilized as solid acid catalyst in organic reactions [4, 5]. Therefore, the modification of starch is rapidly developed along with its growing applications. Starch-based nanoparticles have received a great deal of attention because of their nano-size, large surface area, biodegradable, and good biocompatibility. These characteristics favour the employment of starch nanoparticles in a wide range of various industrial applications especially food products, biomedical fields especially drug carriers, composites filler, water treatment agent, fat replacer and catalytic processes [9-13]. Moreover, starch nanoparticles have raised much attention, as sustainable development policies tend to expand with the decreasing reserve of fossil fuel and the growing concern for the environment [10]. These bio-based nanoparticles have received a

tremendous level of attention as a promising natural material in waste water treatment due to their unique biological and adsorptive properties [11, 12].

In recent times, xanthenes and benzoxanthenes have attracted attention of medicinal chemists as well as organic chemists due to their wide range of biological and pharmacological activities such as antibacterial and anti-inflammatory activities [14], photodynamic therapy and as antagonism for the paralyzing action of zoxazolamine [15]. Moreover, these valuable compounds have found wide usage such as fluorescent dyes [16], in laser technologies [17] and as pH-sensitive fluorescent materials for visualization of biomolecules [18]. Due to the high medicinal and biological importance of xanthenes, several methods have been reported for the synthesis of these heterocycles, which include trapping of benzynes by phenols, cyclodehydrations, condensation between aromatic 2-hydroxyl aldehydes and 2-tetralone and intramolecular phenyl carbonyl coupling reactions of benzaldehyde and acetophenone derivatives. Also, 14-aryl-14*H*-di benzo[a.j]xanthenes and related products have been prepared by the reaction of 2-naphthol with formamide, 2-naphthol-1-methanol and carbon monoxide [19]. On the other hand, a number of methods have been developed for the synthesis of 14-*H*-dibenzo[a,j]xanthene by condensation of 2-naphthol and aldehydes in the presence of strontium sulfamic acid [20], Amberlyst-15 [21], $K_5CoW_{12}O_{40}.3H_2O$ [22], $FeCl_3$ [23], WO_3/ZrOb [24], PS/AlClb [25], Alum [26], $In(OTF)_3$ [27]. Therefore, a significant attention has been focused on designing environmentally benign catalysts and synthetic strategies for the preparation of xanthenes derivatives. The green processes in modern chemical synthesis involve the use of biodegradable, cost-effective and efficient catalysts, non-toxic system such as water, supercritical fluids and the reactions under solvent-free conditions. Advantages of solvent-free reactions include cost savings, energy consumption, atom economy, or improved atom utilization reduced decreased reaction times, and a

considerable reduction in reactor size and simplicity in processing, which are beneficial to the industry as well as to the environment [28].

In the present work, we report a simple and efficient procedure for one-pot synthesis of 14-aryl-14-*H*-dibenzo[a,j]xanthenes using sulfonated starch nanoparticles (HO_3S-SNPs) as an effective, neutral and heterogeneous acidic catalyst under solvent-free conditions (Scheme 1).

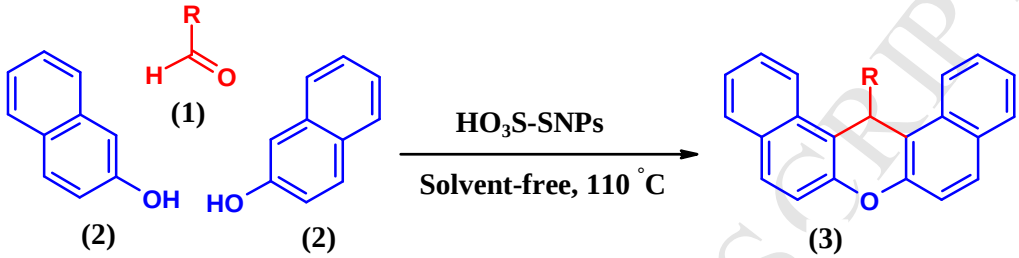

Scheme 1. Synthesis of 14-aryl-14*H*-dibenzo[a,i]xanthenes using HO_3S-SNPs as catalyst.

2. Experimental

Chemical substances were purchased from Merck or Aldrich. Melting points were determined on an Electrothermal 9100 apparatus using open-glass capillary and are uncorrected. FT-IR spectra were recorded as KBr pellets on a Shimadzu FT-IR-8400S spectrometer. ^{1}H NMR (400 MHz) spectra were obtained using a Bruker DRX-400 AVANCE spectrometer. Analytical thin-layer chromatography (TLC) was accomplished on 0.2 mmprecoated plates of silica gel 60 F-254 (Merck) or neutral alumina oxide gel 60F 254 (Merck). Themorphological characteristics of chitosan derivatives were observed by a scanning electron microscope (SEM, LEO 1544VP) operating at an accelerating voltage of 20 kV under high vacuum. Nanostructures were characterized using a Holland Philips Xpert X-ray diffraction (XRD) diffractometer (CuK, radiation, λ= 0.154056 nm), at a scanning speed of 2°/min from 10° to 100° (2θ).

2.1. Synthesis of starch nanoparticles

0.35 g of maleic acid was firstly dissolved in 100 mL of distillated water, then 1 g of starch was added to the this solution the resulted mixture was stirred for 3 h. Then, hydrochloric acid

and sodium hydroxide solution (0.1 M) was dropped slowly into the mixture solution until the pH value was titrated to 4.0 with vigorous mechanical stirring and under continuous Ar atmosphere bubbling for 8 h. Afterwards, 0.054 g of potassium persulfate was added to the mixture and stirred for 2 h at 70 °C under Ar atmosphere. The mixture was cooled in ice-bath and the formed nanoparticles were dried by dry ice.

2.2. Synthesis of sulfonated starch nanoparticles:

HO_3S-SNPs were prepared according to reported procedure in the literature [4]. A 500 mL suction flask was equipped with a pressure equalizing dropping funnel containing chlorosulfonic acid and gas inlet tube for conducting HCl gas over adsorbing the solution water. A flask was charged with starch nanoparticles (500 g) and dispersed in dry $CHCl_3$ (20 mL). Subsequently, chlorosulfonic acid (1.00 g, 9 mmol) was added drop-wise manner to a cooled (ice-bath) solution of starch over a 2 h period, which HCl gas evolved from the reaction vessel immediately. After the addition was completed the mixture was filtered and washed with methanol (30 mL) and dried at room temperature to obtain HO_3S-SNPs (5.06 g) as cream powder. The number of H^+ sites of starch-SO_3H was determined by acid–base titration and found to be 1.50 meq/g of modified starch at 25 $^{\circ}$C. The sulfur content of the samples was determined 1.45 mmol/g by conventional elemental analysis.

2.3. General method for the synthesis of benzoxanthenes

In a glass tube a mixture of aldehyde (1.0 mmol), 2-naphthol (2.0 mmol) and HO_3S-SNPs (0.08 g) were stirred at 110 $^{\circ}$C in an oil bath for the appropriate time, as indicated by TLC for a complete reaction. Ethyl acetate (10 mL) was added and the reaction mixture filtered to separate the catalyst. Pure products were afforded by evaporation of the solvent, followed by recrystallization from ethanol. All the products were characterized by comparison of IR and NMR spectral data with the values of authentic samples.

14-(Phenyl)14*H*-dibenzo[a,j]xanthenes (3a): pale yellow solid; IR (KBr) υ_{max} (cm^{-1}): 3071 (aromatic C–H), 2923 (aliphatic C-H), 1624 (C=C), 1249 (C-O); ^{1}H NMR ($CDCl_3$, 400 MHz) δ (ppm): 6.5 (s, 1H), 6.98-7.01 (t, 1H *J*=7.2 Hz), 7.13 (s, 1H), 7.15-7.17 (d, 1H *J*=8 Hz), 7.39 (s, 1H), 7.41-7.43 (d, 1H, *J*=7.2 Hz), 7.48-7.60 (m, 6H), 7.79-7.84 (m, 4H), 8.39- 8.41 (2H, d, *J*=8 Hz); ^{13}C NMR ($CDCl_3$, 100 MHz) δ (ppm): 148.8, 145.0, 131.5, 131.1, 128.8, 128.5, 128.2 126.8, 126.5, 126.4, 124.2, 122.7, 118.0, 117.4, 38.1.

14-(3-Nitrophenyl)14*H*-dibenzo[a,j]xanthenes (3b): yellow solid; IR (KBr) υ_{max} (cm^{-1}): 3074 (aromatic C–H), 2923 (aliphatic C-H), 1625 (C=C), 1559 (NO_2), 1346 (NO_2), 1249 (C–O); ^{1}H NMR ($CDCl_3$, 400 MHz) δ (ppm): δ= 6.61 (1H, s), 7.29-7.31 (1H, d, *J*=7.2 Hz), 7.44-7.46 (2H, d, *J*=7.2 Hz), 7.51-7.53 (2H, d, *J*=8.4 Hz), 7.62 (2H, t, *J*=8.4 Hz), 7.83-7.85 (6H, m), 8.30-8.32 (2H, d, *J*=7.6 Hz), 8.42 (1H, s); ^{13}C NMR ($CDCl_3$, 100 MHz) δ (ppm): 37.3, 116.3, 116.8, 117.4, 121.1, 122.3, 125.4, 126.9, 128.2, 129.1, 134.7, 136.3, 137.1, 138.2, 146.5, 147.9, 158.3.

14-(4-Nitrophenyl)14*H*-dibenzo[a,j]xanthenes (3c): pale yellow solid; IR (KBr) υ_{max} (cm^{-1}): 3041 (aromatic C–H), 1622 (C=C), 1583, 1548 (NO_2), 1348 (NO_2), 1242 (C–O), 800-850; ^{1}H NMR ($CDCl_3$, 400 MHz) δ (ppm): 6.61 (1H, s), 7.43–7.45 (2H, t, *J*=8.0 Hz), 7.51–7.53 (2H, d, *J*=8.1 Hz), 7.59–7.61(2H, t, *J*=8.0 Hz), 7.68–7.70 (2H, d, *J*=8.1 Hz), 7.84–7.87 (4H, m), 8.00–8.02 (2H, d, *J*=8.0 Hz), 8.28–8-30 (2H, d, *J*=8.0 Hz); ^{13}C NMR ($CDCl_3$, 100 MHz) δ (ppm): 36.9, 115.9, 116.2, 117.1, 120.2, 122.5, 124.8, 126.1, 128.1, 129.7, 132.6, 134.1, 135.9, 148.3, 159.1.

14-(2-Flouro)14*H*-dibenzo[a,j]xanthenes (3d): cream solid; IR (KBr) υ_{max} (cm^{-1}): 3090 (aromatic C–H), 2923 (aliphatic C-H), 1623 (C-C), 1458 (C=C), 1243 (C–O), 1100-1250; ^{1}H NMR ($CDCl_3$, 400 MHz) δ (ppm): 6.79 (1H, s), 6.81–6.83 (1H, d, *J*=6.8 Hz), 6.96-7.04 (2H, m), 7.20–7.24 (3H,m), 7.41–7.62 (4H, m), 7.79–7.84 (4H, m), 8.40-8.42 (2H, d, *J*=8.8 Hz);

^{13}C NMR ($CDCl_3$, 100 MHz) δ (ppm): 30.2, 115.1, 115.2, 116.7, 117.9, 122.3, 124.4, 125.1, 127.1, 128.2, 128.6, 129.1, 130.9, 131.1, 131.5, 132.4.

14-(2-Chlorophenyl)14*H*-dibenzo[a,j]xanthenes (3e): white solid; IR (KBr) υ_{max} (cm^{-1}): 3056 (aromatic C–H), 2924 2992 (aliphatic C-H), 1247 (C-O); ^{1}H NMR ($CDCl_3$, 400 MHz) δ (ppm): 6.80 (1H, s,) 6.89–6.96 (2H, m), 7.25–7.26 (1H, d, *J*=8.4 Hz), 7.38–7.46 (3H, m), 7.49-7.51 (2H, d, *J*=8.8 Hz), 7.61-7.65 (2H, t, J=7.6 Hz), 7.79–7.84 (4H, m), 8.76-8.76 (2H, d, J=8.4 Hz); ^{13}C NMR ($CDCl_3$, 100 MHz) δ (ppm): 36.4, 117.9, 123.3, 124.6, 125.5, 127.8, 128.6, 129.4, 129.5, 131, 132.5, 132.6, 134.5, 141.3, 147.5, 149.8, 152.

14-(4-Chlorophenyl)14*H*-dibenzo[a,j]xanthenes (3f): yellow solid; IR (KBr) υ_{max} (cm^{-1}): 3050 (aromatic C–H), 2922 (aliphatic C-H), 1625 (C-C), 1244 (C-O); ^{1}H NMR ($CDCl_3$, 400 MHz) δ (ppm): 6.48 (1H, s), 7.10–7.12 (2H, d, *J*=7.2 Hz), 7.42–7.50 (6H, m), 7.58–7.61 (2H, t, *J*=7.2 Hz), 7.80–7.86 (4H, m), 8.32–8.34 (2H, d, *J*=8 Hz); ^{13}C NMR ($CDCl_3$, 100 MHz) δ (ppm): 37.39, 116.74, 118.02, 122.42, 124.38, 126.93, 128.65, 128.92, 129.10, 129.50, 131.05, 131.25, 132.08, 143.47, 148.68.

14-(2,4-Dichlorophenyl)14*H*-dibenzo[a.j]xanthenes (3g): pale yellow solid; IR (KBr) υ_{max} (cm^{-1}): 3061 (aromatic C–H), 2923 (alyphatic C-H), 1624 (C-C), 1247 (C-O); ^{1}H NMR ($CDCl_3$, 400 MHz) δ (ppm): 6.75 (1H, s), 6.89-6.91 (1H, t, *J*=6.4 Hz), 7.27-7.31 (2H, m), 7.42-7.49 (4H, m), 7.60-7.64 (2H, t, *J*=8.4 Hz), 7,79-7.84 (4H, t), 8.64-8.66 (2H, d, *J*=8 Hz); ^{13}C NMR ($CDCl_3$, 100 MHz) δ (ppm): 36.6, 117.3, 117.5, 118.4, 123.3, 126.7, 127.5, 128.4, 130.8, 133.5, 135, 141.5, 150.9.

14-(4-Methyl)14*H*-dibenzo[a,j]xanthenes (3h): pale yellow solid, IR (KBr) υ_{max} (cm^{-1}): 3061 (aromatic C–H), 2923 (aliphatic C-H), 1624 (C-C), 1247 (C-O); ^{1}H NMR ($CDCl_3$, 400 MHz) δ (ppm): 2.13 (3H, s), 6.46 (1H,s), 6.95-6.97 (2H,d, *J*=7.6 Hz), 7.39-743 (4H, m), 7.47-7.50 (2H, d, *J*=8.8 Hz), 7.56-7.60 (2H, t, *J*=8Hz), 7.78-7.84 (4H, m), 8.39-8.41 (2H, d, J=8.4 Hz);

^{13}C NMR ($CDCl_3$, 100 MHz) δ (ppm): 20.95, 37.67, 117.48, 118.04, 122.76, 124.25, 126.79, 128.15, 128.81, 128.82, 129.22, 131.11, 131.49, 135.93, 142.18, 148.

14-(2-Methoxy)14*H*-dibenzo[a,j]xanthenes (3i): cream solid, IR (KBr) υ_{max} (cm^{-1}): 3051 aromatic C–H), 2921 (aliphatic C-H), 1622 (C=C), 1247 (C-O); ^{1}H NMR ($CDCl_3$, 400 MHz) δ (ppm): 3.62 (s, 3H, OCH_3), 6.46 (s, 1H, ArH), 6.67-6.69 (2H, d, *J*=8.4 Hz), 7.40-7.44 (4H, m), 7.47-7.49 (2H, d, *J*=8.8 Hz), 7.57-7.60 (2H, t, *J*=7.6 Hz), 7.78-7.84 (4H, m), 8.38-8.40 (2H, d, *J*=8.4 Hz).; ^{13}C NMR ($CDCl_3$, 100 MHz) δ (ppm): 44.11, 55.17, 114.78, 118.59, 119.21, 122.54, 125.23, 127.77, 129.65, 129.72, 130.01, 132.16, 132.76, 137.45, 149.04, 158.

14-(4-Methoxy)14*H*-dibenzo[a,j]xanthenes (3j): pink solid; IR (KBr) υ_{max} (cm^{-1}): 3050 (aromatic C–H), 2922 (aliphatic C-H), 1593 (C=C), 1247 (C-O); ^{1}H NMR ($CDCl_3$, 400 MHz) δ (ppm): 3.62 (3H, s), 6.45 (1H, s), 6.67-6.69 (2H, d, *J*=8.8 Hz), 7.40-7.49 (6H, m), 7.57-7.60 (2H, t, *J*=7.2 Hz), 7.78-7.80 (2H, d, *J*=8.8 Hz), 7.82-7.84 (2H, d, *J*=8.Hz), 8.38-8.40 (2H, d, J=8.4 Hz); ^{13}C NMR ($CDCl_3$, 100 MHz) δ (ppm): 37.11, 55.05, 113.85, 117.54, 118.02, 122.70, 124.23, 126.77, 128.74, 128.82, 129.17, 131.08, 131.43, 137.39, 148.68, 157.21.

14-(3-Hydroxyphenyl)14*H*-dibenzo[a,j]xanthenes (3k): Pale Pink solid; IR (KBr) υ_{max} (cm^{-1}): 3070 (OH), 1595 (C=C), 1246 (C-O); ^{1}H NMR ($CDCl_3$,400 MHz) δ (ppm): 3.45 (s, 3H), 6.45 (s, 1H), 6.33 (d, 1H, *J*=8.2 Hz), 7.08 (t, 2H, *J*=8.4 Hz), 7.21 (d, 1H, *J*=7.5 Hz), 7.33 (t, 2H, *J*=7.2 Hz), 7.52 (d, 2H, *J*=9.0 Hz), 7.58 (t, 2H, *J*=7.6 Hz), 7.72–7.80 (m, 4H), 8.40 (d, 2H, *J*=8.7 Hz); ^{13}C NMR ($CDCl_3$, 100 MHz) δ (ppm): 37.22, 116.05, 118.02,118.75, 123.66, 125.02, 126.45, 130.30, 130.56, 131.03, 131.76, 132.11, 138.54, 149.45, 154.43.

14-(4-Hydroxyphenyl)14*H*-dibenzo[a,j]xanthenes (3l): Pink solid; IR (KBr) υ_{max} (cm^{-1}): 3405 (OH), 1590 (C=C), 1245 (C-O); ^{1}H NMR ($CDCl_3$,400 MHz) δ (ppm): 5.01 (s, 1H, OH), 6.42 (s, 1H, CH), 6.55–8.36 (m,16H, Ar); ^{13}C NMR ($CDCl_3$, 100 MHz) δ (ppm): 37.45, 115.85, 117.85,118.50, 123.20, 124.62, 127.23, 129.30, 129.56, 130.00, 131.58,131.61, 138.02, 149.18, 154.32.

3. Results and discussion

Sulfonic acid-based solid catalysts have used in organic reactions due to their unique properties, such as high reactivity, availability, selectivity, eco-friendly reaction conditions, and ability to promote a wide range of chemical reactions. Since the sulfonation of D-glucose was first reported as a carbohydrate acid catalyst by Hara et al., [29] much efforts have been devoted to developing various types of solid acid catalysts from bio-based polymers, such as sucrose, starch, cellulose and bagasse [30-33] This class of biocompatible and biodegradable catalysts have shown much better performance than commercially available solid acid catalysts, such as Nafion NR50, zeolites and Amerlyst-15 [34]. Furthermore, nanoscale polymers have been attracting more research interest in catalytic systems because of their unique physical and chemical properties, such as nano size, high surface-to-volume ratio and stiffness and improved dispersibility. The polymeric nanoparticles offer a number of distinct advantages over bulk polymers. They have been used in different types of chemical reactions as a suitable support for different catalytic species [35]. In the first of research, starch was modified to starch nanoparticles by a nanoprecipitation process. Next, HO_3S-SNPs were prepared by the reaction of chlorosulfonic acid with starch nanoparticles and the by-product, HCl gas, was easily removed from the reaction vessel (Scheme 2).

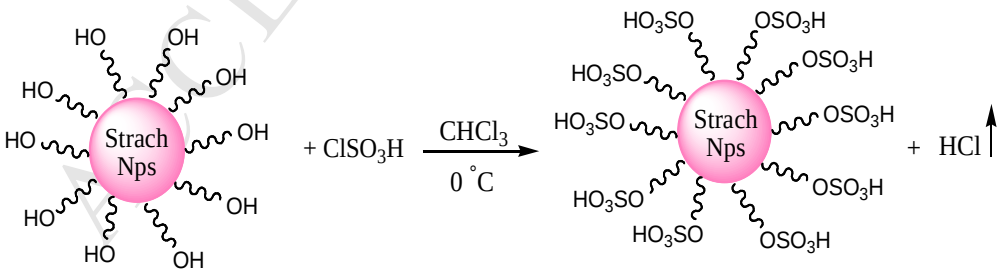

Scheme 2: Preparation steps for fabricating HO_3S-SNPs.

The morphology and structure of starch nanoparticles were investigated by FT-IR, XRD, TEM and SEM. The FT-IR spectrum of starch nanoparticles are shown in Fig. 1. The O-H stretching and the C-H stretching vibration gave strong signals at 3431 and 2924 cm^{-1},

respectively. Meanwhile, the band at 1630 cm^{-1} was ascribed to O-H bending vibration. Besides, several discernible absorbencies at 1154 and 1023 cm^{-1} were assigned to the C-O bond stretching vibrations of glucose units [36].

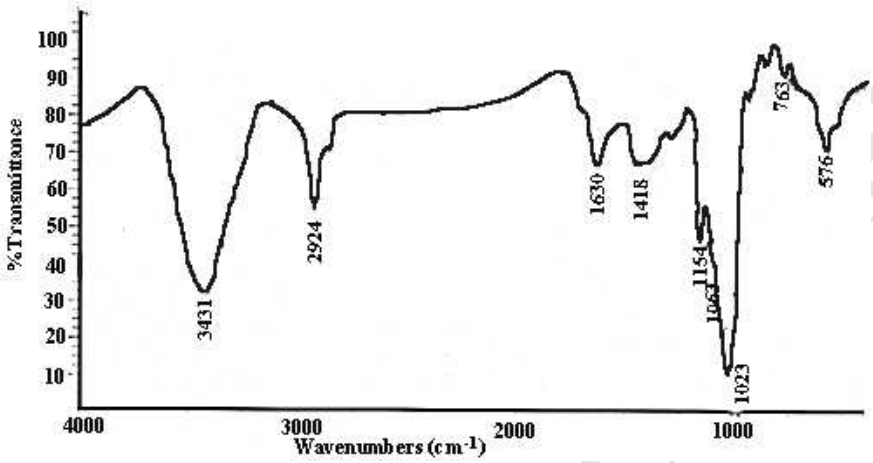

Fig. 1: FT-IR of starch nanoparticles.

Fig. 2 (a) and (b) display XRD result of native starch and starch nanoparticles, respectively. The sharp diffraction peaks at 5.8°, 17.4°, 22.3°, and 24.2° were presented in spectrogram of unmodified starch, which indicated that starch exhibited a typical B-type X-ray pattern. The spectrogram of starch nanoparticles showed a broad peak, suggesting that it was the amorphous nature. Fu et al. also reported the similar XRD results for starch nanoparticles [36].

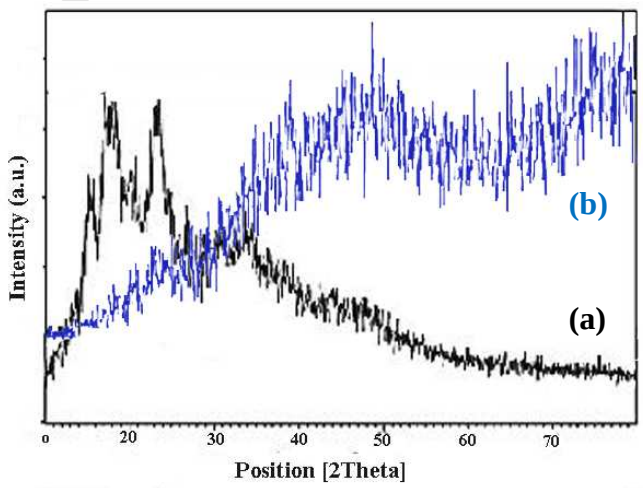

Fig. 2. XRD patterns of (a) starch and (b) starch nanoparticles.

Fig. 3 presents the XRD-diffraction patterns of the HO_3S-SNPs. The same broad peak was observed in XRD pattern of HO_3S-SNPs, indicating retention of the amorphous nature of the starch nanoparticles during the sulfonation process.

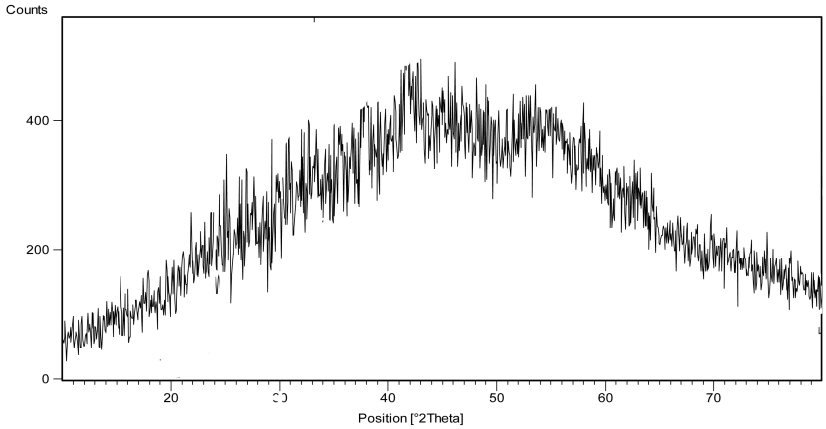

Fig. 3. XRD pattern of HO_3S-SNPs.

Fig. 4 (a) and (b) showed SEM and TEM micrographs of starch nanoparticles, respectively. SEM in Fig. 4(a) shows the surface morphology of the starch nanoparticles. TEM image in Fig. 4(b) indicates that the particles are nearly spherical and they have a range diameter of 50-80 nm. SEM image for HO_3S-SNPs in Fig. 4(c), shows significant difference between starch nanoparticles and sulfonated starch. After sulfonation of the starch nanoparticles, the aggregates were foliated with rougher surfaces.

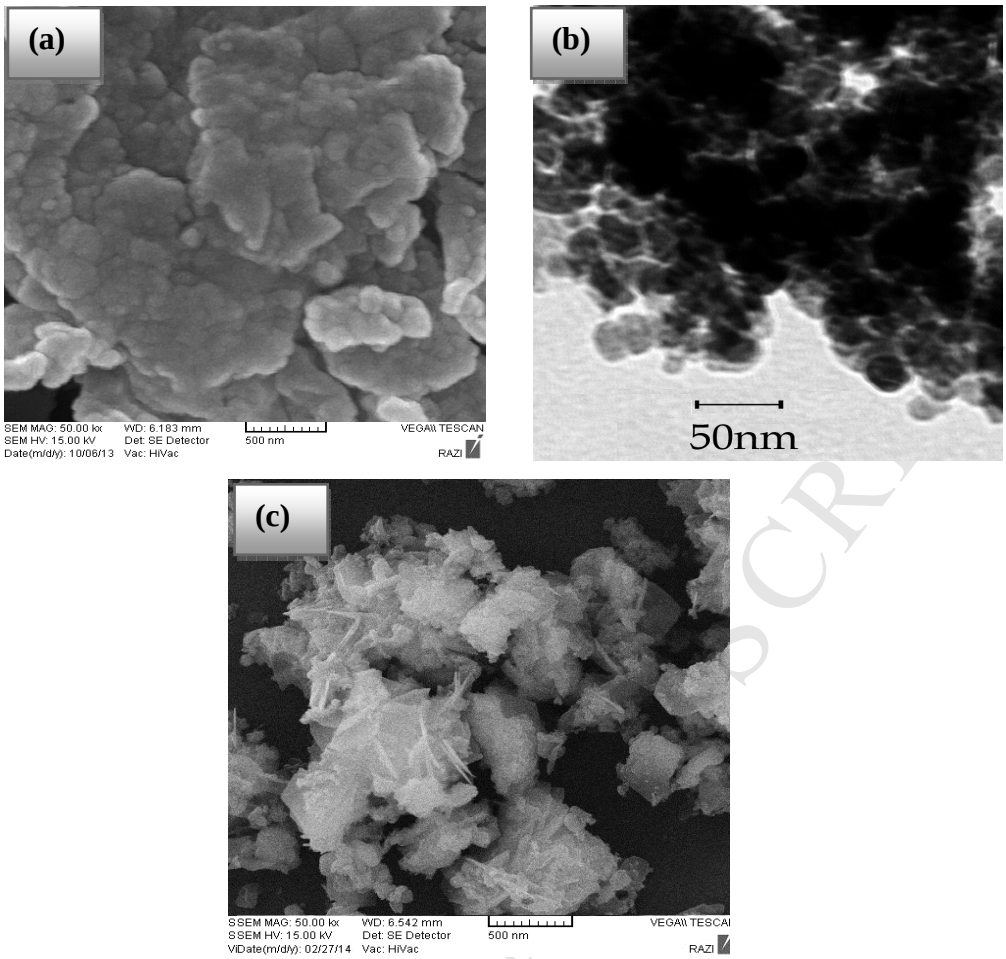

Fig. 4. (a) SEM and (b) TEM image of starch nanoparticles and (c) SEM of HO_3S-SNPs.

To investigate the feasibility of the synthetic methodology for the synthesis of benzoxanthenes, initial experiments were performed by using 2-naphthol and benzaldehyde as reactants at 110 °C under solvent-free conditions. Initially, the Starch-SO_3H was studied for its activity in the model reaction. The results showed that 0.08 g of catalyst was optimal for this reaction (Table 1, Entry 4). In a blank experiment no desired product was observed under similar reaction conditions in the absence of acidic catalyst (Table 1, Entry 1). In the next stage for getting the best conditions, we carried out a model study with the same reagent system at 90°C, 100°C, 110°C and 120°C temperatures, (Table 1, Entries, 4 and 8-11). Increasing the temperature enhances the reaction rate substantially with respective 70%, 85%, 92% and 80% yield. According to the results, we obtained the best results at 110 °C, and therefore all the reactions were performed at this temperature for the synthesis of 14-aryl-14-

H-dibenzo[a,j]xanthenes. The reaction time was still long and needs to be improved and for this reason, HO_3S-SNPs were used in this organic reaction. It was observed that SO_3H-SNP is better than the Starch-SO_3H tested in this study in terms of reaction yield (92%) and reaction time (45 min) (Table 1, entry 13). Some solvents such as EtOH, MeOH, CH_3CN, H_2O and CH_2Cl_2, did not show improvement in the yield of product (Table 1, Entries 14-18).

Table 1. Results of screening the conditions.

Entry	Catalyst	Catalyst(g)	Solvent	Temp (°C)	Time (min)	Yield (%)
1	-	-	Solvent-free	110	240	-
2	Starch	0.08	Solvent-free	110	240	-
3	Starch NPs	0.08	Solvent-free	110	240	-
4	Starch-SO_3H	0.08	Solvent-free	110	105	90
5	Starch-SO_3H	0.05	Solvent-free	110	180	75
6	Starch-SO_3H	0.01	Solvent-free	110	210	70
7	Starch-SO_3H	0.1	Solvent-free	110	105	84
8	Starch-SO_3H	0.15	Solvent-free	110	105	81
9	Starch-SO_3H	0.08	Solvent-free	120	105	80
10	Starch-SO_3H	0.08	Solvent-free	100	180	85
11	Starch-SO_3H	0.08	Solvent-free	90	180	70
12	Starch-SO_3H	0.08	Solvent-free	r.t.	240	-
13	HO_3S-SNPs	0.08	Solvent-free	110	45	92
14	HO_3S-SNPs	0.08	EtOH	Reflux	120	65
15	HO_3S-SNPs	0.08	MeOH	Reflux	120	58
16	HO_3S-SNPs	0.08	CH_3CN	Reflux	120	70
17	HO_3S-SNPs	0.08	CH_2Cl_2	Reflux	120	35
18	HO_3S-SNPs	0.08	H_2O	Reflux	120	40

Under the optimized reaction conditions, a series of aldehydes with 2-naphthol were explored in the presence of HO_3S-SNPs. The results were summarized in Table 2. The procedure was highly effective for the preparation of 14-aryl-14-*H*-dibenzo[a,j]xanthenes. As expected, the aromatic aldehyde substrates containing electron donor groups (such as OMe and OH), showed weaker results than the cases containing electron withdrawing groups (such as NO_2, Cl).

Table2. Synthesis of 14-aryl-14-*H*-dibenzo[a,j]xanthenes using HO_3S-SNPs.

Entry	R	Product	SO_3H-SNPs		M.p (ºC)		Ref
			Time(min)	Yield(%)[a]	(Found)	(Reported)	
1	C_6H_5	3a	45	92	183-185	181-183	37
2	3-$NO_2C_6H_4$	3b	40	95	208-210	211-212	38
3	4-$NO_2C_6H_4$	3c	30	97	310-312	310-312	38
4	2-FC_6H_4	3d	40	95	209-210	211-212	38
5	2-ClC_6H_4	3e	45	92	213-215	214-215	39
6	4-ClC_6H_4	3f	35	95	287	287-289	37
7	2,4-ClC_6H_4	3g	30	95	252-253	254-255	40
8	4-$CH_3C_6H_4$	3h	70	95	226	227-230	41
9	2-$OCH_3C_6H_4$	3i	80	91	263-265	263-265	41
10	4-$OCH_3C_6H_4$	3j	70	94	203-204	202–204	42
11	3-OHC_6H_4	3k	70	90	241-242	240-241	42
12	4-OHC_6H_4	3l	70	92	139-140	138-140	42

[a] Isolated yields

The formation of benzoxanthenes from aldehyde derivatives and 2-naphthol in the presence of HO_3S-SNPs as catalyst can be explained by a tentative mechanism is presented in Scheme 3. HO_3S-SNP is supposed as a Lewis acid catalyst to facilitate the activation of the aldehyde. The acidic SO_3H groups distributed on the surface of starch nanoparticles in high concentrations activate the carbonyl group of the aldehyde. Then, one molecule of 2-naphthol condense with an activated aldehyde (I) to provide intermediate (II), which can be regarded as a fast Knoevenagel addition. In the next step, the active methylene of the second molecule of 2-naphthol react with intermediate (II) *via* conjugate Michael addition to produce the intermediate (III), which undergoes intramolecular cyclodehydration to furnish the desired 14-aryl-14-*H*-dibenzo[a,j]xanthenes (V) [42, 43].

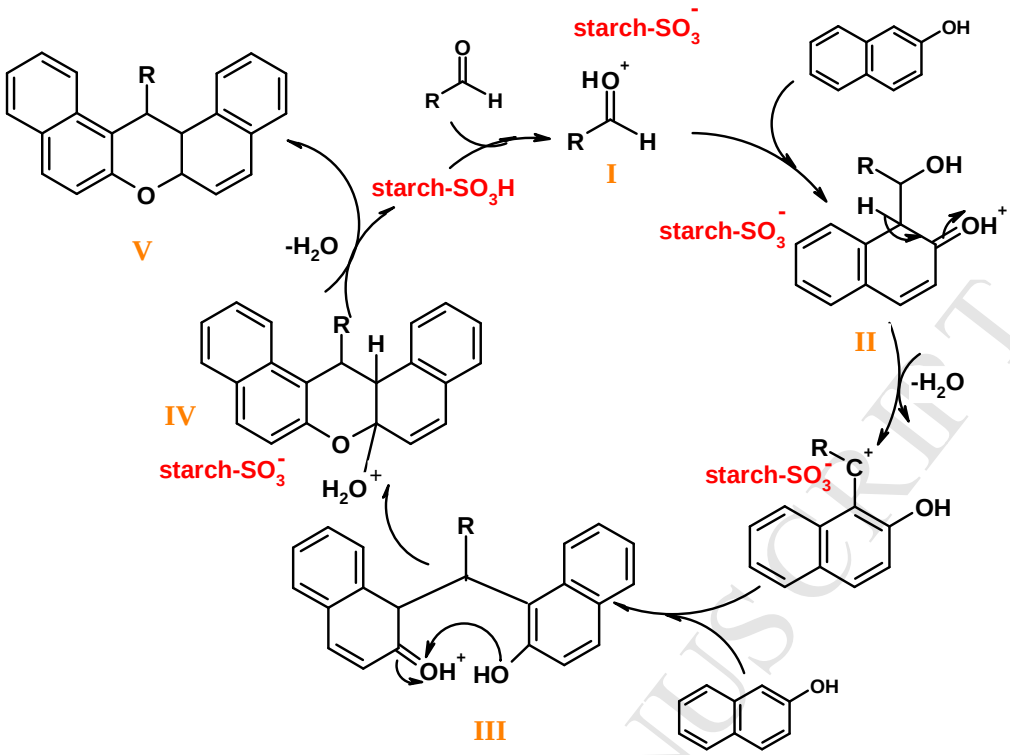

Scheme.3: Proposed reaction mechanism.

To have a better understanding of the performance of our catalytic system, the effectiveness of the SO_3H-SNPs was also compared to that of catalysts reported previously in the synthesis of 14-aryl-14-*H*-dibenzo[a,j]xanthenes from the reaction of 2-naphthol and various aromatic aldehydes and the results are listed in Table 3. As can be seen in this table, the present catalyst was found to be the most efficient catalyst among all of the catalysts in the literatures. The reaction in the presence of HO_3S-SNPs was indicated a lot of significant such as; simplicity of the reaction, excellent yields, low reaction times, naturally safe, biodegradable, economical, and eco-friendly catalyst. These advantages can be related to the highly activity due to its nanoporosity and high surface area.

Table 3: The synthesis of 3a using different catalysts.

Entry	Catalyst	Time (min)	Yield(%)[a]	Temp (°C)	Ref.
1	HO_3S-SNPs	45	92	110	This research
2	Dowex-50 W	160	84	100	22
3	TCCA	50	74	110	44

4	Iodine	18	85	90	45
5	$H_5PW_{10}V_2O_{40}$	60	92	100	46
6	H_2SO_4/SiO_2	60	97	125	47
7	PFPAT	189	96	r.t.	48
8	Cellulose sulfuric acid	120	90	110	49
9	SBA-15-SO_3H	24h	91	85	50
10	Sulfamic acid	8h	93	125	20
11	AgBr	90	50	140	41
12	AgI	70	70	140	41
13	CuCl	120	40	140	41
14	NiO	140	45	140	41
15	CaO	160	50	140	41
16	AgI-nano	40	92	140	41
17	SBA-15-CO_2H	6h	80	r.t	43
18	MCM-41-SO_3H	60	90	r.t	43

[a] Isolated yields

The reusability of the HO_3S-SNPs was tested for the model reaction. The separated catalyst was used several times and loss of catalytic activity was not observed (Fig. 5).

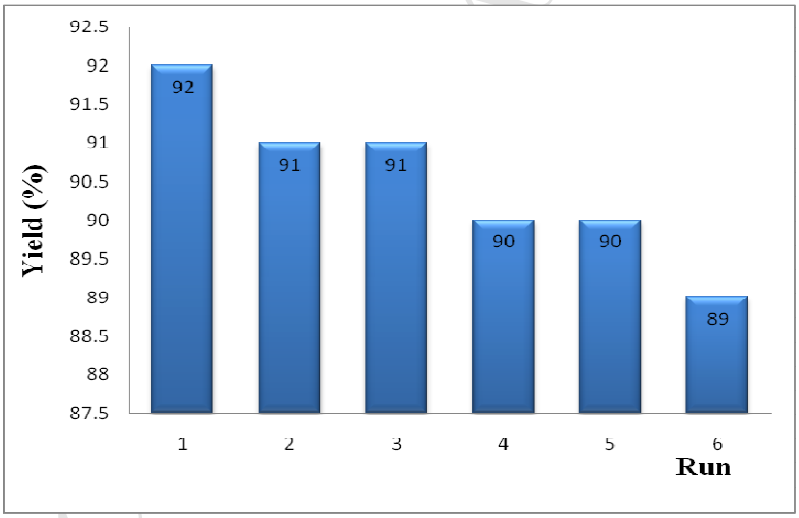

Fig. 5. Recoverability of HO_3S-SNPs.

Conclusions

In summary, the present work was the first report on using HO_3S-SNPs as a novel and very promising solid acid catalyst for the synthesis of 14-aryl-14-*H*-dibenzo[a,j]xanthenes. The application of starch-SO_3H as a highly efficient, inexpensive, easy work-up, and natural solid acid catalyst makes the present methodology economically and eco-friendly acceptable.

Moreover, solvent free, low-cost, non-toxicity, high yields of the desired benzoxanthenes and short reaction times are supporting the protocol toward the green chemistry. Further applications of these biopolymer catalysts are currently under investigation in our laboratory.

Acknowledgments

We gratefully acknowledge the financial support from the Research Council of the University of Kashan for supporting this work by Grant No. (363022/16).

References

[1] K. Nakajima, M. Hara, Amorphous carbon with SO_3H groups as a solid Brønsted acid catalyst, ACS Catal. 2 (2012) 1296−1304.

[2] J. Safari, Z. Zarnegar, A magnetic nanoparticle-supported sulfuric acid as a highly efficient and reusable catalyst for rapid synthesis of amidoalkyl naphthols. J. Mol. Catal. A: Chem. 379 (2013) 269-276.

[3] J. Safari, Z. Zarnegar, An environmentally friendly approach to the green synthesis of azo dyes in the presence of magnetic solid acid catalysts. RSC Adv. 5 (2015) 17738-17745.

[4] A. Shaabani, A. Rahmati, Z. Badri, Sulfonated cellulose and starch: New biodegradable and renewable solid acid catalysts for efficient synthesis of quinolines, Catal. Commun. 9 (2008) 13–16.

[5] I.M. Lokman, U. Rashid, Y.H. Taufiq-Yap, Meso and macroporous sulfonated starch solid acid catalyst for esterification of palm fatty acid distillate, Arab. J. Chem. (2015) doi:10.1016/j.arabjc.2015.06.034

[6] E. Rafiee, M. Khodayari, Synthesis and characterization of a green composite of $H_3PW_{12}O_{40}$ and starch-coated magnetite nano particles as a magnetically-recoverable nano catalyst in Friedel-Crafts alkylation J. Mol. Catal. A: Chem. 398 (2015) 336-343.

[7] S. Chancharoenrith, C. Kamonsatikul, M. Namkajorn, S. Kiatisevi, E. Somsook, Iron oxide/cassava starch-supported Ziegler–Natta catalysts for in situ ethylene polymerization, Carbohydr. Polym. 117 (2015) 319-323.

[8] S. Chakraborty, B. Sahoo, I. Teraoka, L.M. Miller, R.A. Gross, Enzyme-catalyzed regioselective modification of starch nanoparticles, Macromolecules 38 (2005) 61-68.

[9] X. Li, Y. Qin, C. Liu, S. Jiang, L. Xiong, Q. Sun, Size-controlled starch nanoparticles prepared by self-assembly with different green surfactant: The effect of electrostatic repulsion or steric hindrance, Food Chem. 199 (2016) 356–363.

[10] C. Liu, Y. Qin, X. Li, Q. Sun, L. Xiong, Z. Liu, Preparation and characterization of starch nanoparticles viaself-assembly at moderate temperature, Int. J. Biol. Macromol. 84 (2016) 354–360

[11] Q. Chen, H. Yu, L. Wang, Z. Abdin, Y. Chen, Ju. Wang, W. Zhou, X. Yang, R.U. Khan, H. Zhang, X. Chen, Recent progress in chemical modification of starch and its applications, RSC Adv. 5 (2015) 67459-67474.

[12] H.Y. Kim, S.S. Park, S.T. Lim, Preparation, characterization and utilization of starch nanoparticles, Colloids Surf., B Biointerfaces. 126 (2015) 607–620.

[13] S. Chairam, W. Konkamdee, R. Parakhun, Starch-supported gold nanoparticles and their use in 4-nitrophenol reduction J. Saudi Chem. Soc. (2015), doi:10.1016/j.jscs.2015.11.001

[14] (a) A.N. Dadhania, V.K. Patel, D.K. Raval, Catalyst-free sonochemical synthesis of 1,8-dioxo-octahydroxanthene derivatives in carboxy functionalized ionic liquid, C. R. Chim. 15 (2012) 378–383; (b) J.P. Poupelin, G. Saint-Ruf, O. Foussard-Blanpin, G. Narcisse, G.

Uchida-Ernouf, R. Lacroix, Synthesis and anti-inflammatory properties of bis (2-hydroxy-1-naphthyl)methane derivatives I, Eur. J. Med. Chem. 13 (1978) 67–71.

[15] (a) R.M. Ion, The photodynamic therapy of cancer-a photosensitization or a photocatalytic process, Prog. Catal. 2 (1997) 55-76; (b) R. M.Ion, D. Frackowiak, A. Planner, K. Wiktorowicz, he incorporation of various porphyrins into human blood cells, Acta Biochim. Pol. 45 (1998) 833-845.

[16] M. Bass, T.F. Deutsch, M.J. Weber, Frequency and time dependence gain dye solution laser, Appl. Phys. Lett. 13 (1968) 120–124.

[17] M. Ahmad, T.A. King, D. Ko, B.H. Cha, J. Lee, Performance and photostability of xanthene and pyrromethene laser dyes in sol-gel phases, J. Phys. D: Appl. Phys. 35 (2002)1473–1476.

[18] C.G. Knight, T. Stephens, Xanthene-dye-labelled phosphatidylethanolamines as probes of interfacial pH. Studies in phospholipid vesicles, Biochem. J. 258 (1989) 683–689.

[19] (a) D.W. Knight, P.B. Little, The first high-yielding benzyne cyclisation using a phenolic nucleophile: a new route to xanthenes, Synlett (1998) 1141-1143; (b) D.W. Knight, P.B. Little, The first efficient method for the intramolecular trapping of benzynes by phenols: a new approach to xanthenes, J. Chem. Soc., Perkin Trans. (2001) 1771-1777; (c) A. Bekaert, J. Andrieux, M. Plat, New total synthesis of bikaverin, Tetrahedron Lett. 33 (1992) 2805-2806; (d) A. Jha, J. Beal, Convenient synthesis of 12*H*-benzo[a]xanthenes from 2-tetralone, Tetrahedron Lett. 45 (2004) 8999-9001; (e) C.W. Kuo, J.M. Fang, Action of formamide and formanilide on naphthols and on barbituric acid, Synth. Cimmarusti, R. Gazz. Chim. Ital. 77 (1947) 142-143; (f) R.N. Sen, N.J. Sarkar, The condensation of primary alcohols with resorcinol and other hydroxy aromatic compounds, Am. Chem. Soc. 47 (1925) 1079-1071; (g) K. Ota, T. Kito, An improved synthesis of dibenzoxanthene, Bull. Chem. Soc. Jpn. 49 (1976) 1167–1168; (h) C.W. Kuo, J.M. Fang, Synthesis of

xanthenes, indanes, and tetrahydronaphtalenes via intramolecular phenyl–carbonyl coupling reactions, Synth. Commun. 31 (2001) 877-892.

[20] B. Rajitha, B. Sunil Kumar, Y. Thirupathi Reddy, P. Narsimha Reddy, N. Sreenivasulu, Sulfamic acid: a novel and efficient catalyst for the synthesis of aryl-14*H*-dibenzo[a,j] xanthenes under conventional heating and microwave irradiation, Tetrahedron lett. 46 (2005) 8691-8693.

[21] L. Nagarapu, S. Kantevari, V.C. Mahankhali, S. Apuri, Potassium dodecatungsto cobaltate trihydrate ($K_5CoW_{12}O_{40}$:$3H_2O$): A mild and efficient reusable catalyst for the synthesis of aryl-14*H*-dibenzo [aj] xanthenes under conventional heating and microwave irradiation, Catal. Commun. 8 (2007) 1173-1177.

[22] S. Ko, C.F. Yao, Heterogeneous catalyst: Amberlyst-15 catalyzes the synthesis of 14-substituted-14*H*-dibenzo[a,j] xanthenes under solvent-free conditions, Tetrahedron lett. 47 (2006) 8827-8829.

[23] B. Wang, D. Fang, H.L. Wang, X.L. Zhou, Z.L. Liu, $FeCl_3$-Catalyzed condensation of 2-naphthol and aldehydes under solvent-free reaction conditions: An efficient and green alternative for the synthesis of 14-aryl (alkyl)-14-*H*-dibenzo [a,j] xanthenes, Chin. J. Chem. 28 (2010) 2463-2468.

[24] L. Nagarapu, M. Baseeruddin, N.V. Kumari, S. Kantevari, A.P. Rudradas, Efficient synthesis of aryl-14*H*-dibenzo[a,j]xanthenes using $NaHSO_4$–SiO_2 or 5 %WO_3/ZrO_2 as heterogeneous catalysts under conventional heating in a solvent-free media, Synth. Commun. 37 (2007) 2519-2525.

[25] (a) A. Rahmatpour, An efficient, high yielding and ecofriendly method for the synthesis of 14-aryl- or 14-alkyl- 14*H*-dibenzo[a,j]xanthenes using polyvinyl sulfonic acid as a recyclable Brønsted acid catalyst, Monatsh. Chem. 142 (2011) 1259–1263; (b) A. Rahmatpour, J. Aalaie, Polystyrene-supported aluminium chloride: An efficient and

recyclable green catalysfor one-pot synthesis of 14-aryl or alkyl-14*H*-dibenzo[a,j] xanthenes, Heteroat. Chem. 22 (2011) 51–54.

[26] (a) M. Dabiri, M. Baghbanzadeh, M.S. Nikcheh, E. Arzroomchilar, Eco-friendly and efficient one-pot synthesis of alkyl- or aryl-14*H*-dibenzo[a,j]xanthenes in water, Bioorg. Med. Chem. Lett. 18 (2008) 436–438; (b) M. Dabiri, S.C. Azimi, A. Bazgir, One-pot synthesis of xanthene derivatives under solvent-free conditions, Chem. Pap. 62 (2008) 522–526.

[27] S. Urinda, D. Kundu, A. Majee, A. Hajra, Indium triflate-catalyzed one-pot synthesis of 14-alkyl or aryl-14*H*dibenzo[a,j]xanthenes in water, Heteroat. Chem. 20 (2009) 232–234.

[28] J. Safari, Z. Zarnegar, Brønsted acidic ionic liquid based magnetic nanoparticles: a new promoter for the Biginelli synthesis of 3,4-dihydropyrimidin-2(1*H*)-ones/thiones, New J. Chem. 38 (2014) 358-365.

[29] M. Toda, A. Takagaki, M. Okamura, J.N. Kondo, S. Hayashi, K. Domen, M. Hara, Default green chemistry: biodiesel made with sugar catalyst, Nature 438 (2005) 178–178.

[30] V. Budarin, J.H. Clark, J.J.E. Hardy, R. Luque, M.K. ilkowski, S.J. Tavener, A.J. Wilson, Starbons: New starch-derived mesoporous carbonaceous materials with tunable properties, Angew. Chem. Int. Ed. 45 (2006) 3782–3786.

[31] W.Y. Lou, Q. Guo, W.J. Chen, M.H. Zong, H. Wu, T.J. Smith, A highly active bagasse-derived solid acid catalyst with properties suitable for production of biodiesel, Chem. Sus. Chem. 5 (2012) 1533–1541.

[32] M. Hara, Biomass conversion by a solid acid catalyst, Energy Environ. Sci. 3 (2010) 601–607.

[33] B.V. Subba Reddy, A. Venkateswarlu, Ch. Madan, A. Vinu, Cellulose-SO_3H: an efficient and biodegradable solid acid for the synthesis of quinazolin-4(1*H*)-ones, Tetrahedron Lett. 52 (2011) 1891-1894.

[34] W. Chen, X. Peng, L. Zhong, Y. Li, R. Sun, Lignosulfonic acid: A renewable and effective biomass-based catalyst for multicomponent reactions, ACS Sustainable Chem. Eng. 3 (2015) 1366–1373.

[35] J. Safari, F. Azizi, M. Sadeghi, Chitosan nanoparticles as a green and renewable catalyst in the synthesis of 1,4-dihydropyridine under solvent-free conditions, New J. Chem. 39 (2015) 1905-1909.

[36] X. Wang, H. Chen, Z. Luo, X. Fu, Preparation of starch nanoparticles in water in oil microemulsion system and their drug delivery properties, Carbohydr. Polym. 138 (2016) 192–200.

[37] H.R. Shaterian, M. Ghashang, A. Hassankhani, One-pot synthesis of aryl 14*H*-dibenzo [a,j] xanthene leuco-dye derivatives, Dyes. Pigments. 76 (2008) 564-568.

[38] J. Safaei-Ghomi, M.A. Ghasemzadeh, An efficient multi-component synthesis of 14-aryl-14H-dibenzo[a,j]xanthene derivatives by AgI nanoparticles, J. Saudi Chem. Soc. 19 (2015) 642-649.

[39] F.K. Behbahani, M. Valiallahi, Synthesis of 14-aryl-14*H*dibenzo [a,j] xanthenes using $CuSO_4.5H_2O$ as a green and reusable catalyst, Arab. J. Chem. (2013) DOI: 10.1016/j. arabjc.2013.06.014.

[40] S. Rostamizadeh, N. Shadjou, A.M. Amani, S. Balalaie, Silica supported sodium hydrogen sulfate ($NaHSO_4$-SiO_2): A mild and efficient reusable catalyst for the synthesis of aryl-14*H*dibenzo [a,j] xanthenes under solvent-free conditions, Chin. Chem. Lett. 19 (2008) 1151-1155.

[41] H. Naeimi, Z.S. Nazifi, Convenient synthesis of 14-aryl-14-*H*-dibenzo [a,j] xanthenes catalyzed by acyclic Brønsted acidic ionic liquid $[H\text{-}NMP]^+[HSO_4]^-$ under Microwave irradiation, J. Chin. Chem. Soc. 60 (2013) 1113–1117.

[42] H. Naeimi, Z.S. Nazifi, Sulfonated diatomite as heterogeneous acidic nanoporous catalyst forsynthesis of 14-aryl-14-*H*-dibenzo[a,j]xanthenes under green conditions, Appl. Catal. A: Gen. 477 (2014) 132–140.

[43] J. Mondal, M. Nandi, A. Modak, A. Bhaumik, Functionalized mesoporous materials as efficient organocatalysts for the syntheses of xanthenes, J. Mol. Catal. A: Chem. 363–364 (2012) 254–264.

[44] B. Maleki, M. Gholizadeh, Z. Sepehr, 1,3,5-Trichloro-2,4,6-triazinetrion: a versatile heterocycle for the one-pot synthesis of 14-aryl- or alkyl -14*H*-dibenzo[a,j]xanthene, 1,8-dioxooctahydroxanthene and 12-aryl-8,9,10,12-tetrahydrobenzo[a]xanthene-11-one derivatives under solvent-free conditions, Bull. Korean Chem. Soc. 32 (5) (2011)1697–1702.

[45] G.H. Mahdavinia, S. Rostamizadeh, A.M. Amani, Z. Emdadi, Ultrasound-promoted greener synthesis of aryl-14-H-dibenzo[a,j]xanthenes catalyzed by $NH_4H_2PO_4/SiO_2$ in water, Ultrason. Sonochem.16 (2009) 7–10.

[46] R. Tayebee, S. Tizabi, Highly Efficient and environmentally friendly preparation of 14-aryl-14*H* dibenzo[a,j]xanthenes catalyzed by tungsto-divanado-phosphoric acid, Chinese J. Catal. 33 (2012) 962–969.

[47] G.B. Dharma Rao, M.P. Kaushik, A.K. Halve, An efficient synthesis of naphtha[1,2-e]oxazinone and 14-substituted-14*H*-dibenzo[a,j]xanthene derivatives promoted by zinc oxide nanoparticle under thermal and solvent-free conditions, Tetrahedron Lett. 53 (2012)2741–2744.

[48] S. Khaksar, N. Behzadi, Mild and Highly Efficient method for synthesis of 14-aryl(alkyl)-14*H*-dibenzo[a,j]xanthenes and 1,8-dioxooctahydroxanthene derivatives using pentafluorophenyl ammonium triflate as a novel organocatalyst, Chinese J. Catal. 33 (2012) 982–985.

[49] J. Venu Madhava, Y. Thirupathi Reddy, P. Narsimha Reddy, M. Nikhil Reddy, S. Kuarma, P.A. Crooksb, B. Rajitha, Cellulose sulfuric acid: An efficient biodegradable and recyclable solid acid catalyst for the one-pot synthesis of aryl-14*H*-dibenzo[a.j]xanthenes under solvent-free conditions, J. Mol. Catal. A: Chem. 304 (2009) 85–87.

[50] M.A. Naik, D. Sachdev, A. Dubey, Sulfonic acid functionalized mesoporous SBA-15 for one-pot synthesis of substituted aryl-14*H*-dibenzo xanthenes and bis(indolyl) methanes, Catal. Commun. 11 (2010) 1148–1153.

Figure captions

Table 1. Results of screening the conditions.

Table2. Synthesis of 14-aryl-14-*H*-dibenzo[a,j]xanthenes using SO_3H-SNPs.

Table 3: The synthesis of 3a using different catalysts.

Scheme 1. Synthesis of 14-aryl-14*H*-dibenzo[a,i]xanthenes using SO_3H-SNPs as catalyst.

Scheme 2: Preparation steps for fabricating SO_3H-SNPs.

Scheme.3: Proposed reaction mechanism.

Fig. 1: FT-IR of starch nanoparticles.

Fig. 2. XRD patterns of (a) starch and (b) starch nanoparticles.

Fig. 3. XRD pattern of SO_3H-SNPs.

Fig. 4. (a) SEM and (b) TEM image of starch nanoparticles and (c) SEM of SO_3H-SNPs.

Fig. 5. Recoverability of SO_3H-SNPs.